

Facile synthesis of microporous sulfur-doped carbon spheres as electrodes for ultrasensitive detection of ascorbic acid in food and pharmaceutical products

Mohammed Y. Emran,^{a,b} Mohammed A. Shenashen,^a Adel A. Abdelwahab,^b Mohamed Abdelmottaleb,^b Sherif A. El-Safty,^{a,c}

^aNational Institute for Materials Science (NIMS), 1-2-1 Sengen, Tsukuba-shi, Ibaraki-ken, 305-0047, Japan

^bDepartment of Chemistry, Faculty of Science, Al-Azhar University, Assiut 71524, Egypt.

^cFaculty of Engineering and Advanced Manufacturing, University of Sunderland, Sunderland SR6 0DD, UK.

*E-mail: sherif.elsafty@nims.go.jp & sherif.el-safty@sunderland.ac.uk

Supplementary materials

1-Experimental

1.1 Materials

All chemicals were of analytical grade and were used without further purification. Sodium Dopamine hydrochloride, uric acid (UA), Glucose (Gl) and potassium ferricyanide [K₃Fe(CN)₆], human blood serum, and potassium chloride (KCl) were purchased from Sigma–Aldrich Company, Ltd., USA. L(+)-ascorbic acid (AA), disodium hydrogen phosphate (Na₂HPO₄), citric acid, sodium dihydrogen phosphates (NaH₂PO₄), sodium carbonate (Na₂CO₃), sodium chloride (NaCl), potassium sulfate (K₂SO₄), sodium hydrogen sulfate (NaHSO₄), thiourea and H₂O₂ (30%) were purchased from Wako Company, Ltd., Osaka, Japan.

1.2 Fabrication of working electrode

A dispersed solution of working materials was prepared as follows; 5 mg of S-MCMS-700, S-MCMS-800, and S-MCMS-900 were dispersed in 1 mL Milli-Q water and further used for electrode modifications. The glassy carbon electrode (GCE, diameter 4.0 mm) was

successively polished to a mirror using 0.05 μM alumina slurry, then diamond slurry with washing by deionized water every sweep, after that it sonicated in acetone and double-distilled water, and dried at room temperature. The electrode design was fabricated by drop casting of 20 μL of S-MCMS-700, S-MCMS-800, and S-MCMS-900 onto the surface of GCE and dried at room temperature

1.3 Electrochemical sensing system

Zennium/ZAHNER-Elektrik instrument that was controlled by Thales Z 2.0 software at room temperature was used for all electrochemical measurements. A conventional three-electrode system containing GCE (3 mm) as working electrodes, platinum wires as a counter electrode, and Ag/AgCl (3 M NaCl) as a reference electrode were used for electrochemical analysis. The modified electrode was activated under continuous cyclic voltammetric sweep for 10 cycles from 0.0 to 2 V at scan rate 100 mVs^{-1} in 0.1 M PBS (pH 6.4).

1.4 Characterization analyses

The morphology of the annealed sample was investigated by FE-SEM (JEOL Model 6500) at 20 kV. Analysis material was fixed onto the FE-SEM stage using carbon tape before insertion into the FE-SEM chamber. The ion sputter (Hitachi E-1030) was used to deposit thin-layered Pt films on electrodes at 25 $^{\circ}\text{C}$.

The surface properties of the material involving the pore structure distribution and surface area were estimated by N_2 adsorption at 77 K using a BELSORP36 analyzer (JP. BEL Co., Ltd.). The samples were thermally treated at 200 $^{\circ}\text{C}$ for at least 6 h under N_2 atmosphere. The specific surface area (SBET) was calculated using the Brunauer–Emmett–Teller (BET) method with multipoint adsorption data from the linear section of the N_2 adsorption isotherm. The pore size distribution was determined using nonlocal DFT (NLDFT).

The structural geometry of the catalyst was further examined by WA-XRD. The WA-XRD patterns were recorded using an 18 kW diffractometer (Bruker D8 Advance) at a scan rate of $10^{\circ}/\text{min}$ with monochromated $\text{CuK}\alpha$ -X-radiation ($\lambda = 1.54178 \text{ \AA}$). The DIFRAC plus Evaluation Package (EVA) software with the PDF-2 Release 2009 databases provided by Bruker AXS was used to analyze the diffraction and structure analysis diffraction data. The TOPAS package program was applied to integrate several types of X-ray diffraction (XRD) analyses.

XPS analysis was conducted on a PHI Quantera SXM (ULVAC-PHI) instrument (Perkin–Elmer Co., USA) equipped with Al $\text{K}\alpha$ as an X-ray source for excitation ($1.5 \text{ mm} \times 0.1 \text{ mm}$,

15 kV, 50 W) under a pressure of 4×10^{-8} Pa. A thin film of the sample was deposited on a Si slide before the start of analysis.

Raman spectroscopy (HR Micro Raman spectrometer, Horiba, Jubin Yvon) was conducted using an Ar ion laser at 633 nm. A CCD (charge coupled device) camera detection system and the LabSpec-3.01C software package were used for data acquisition and analysis, respectively. To ensure the accuracy and precision of the Raman spectra, 10 scans of 5 s at from 450 cm^{-1} to 2900 cm^{-1} were recorded.

2. Results and discussion

2.1 pH-dependent AA behavior on S-MCMS-900-modified electrode

One of the factors that affect electrochemical reaction is the pH-supporting electrolyte solution. The pH effect of AA (0.5 mM) on the S-MCMS-900-modified electrode was studied using CV in 0.1 mM PBS from pH 5 to 7.4 at a scan rate of 100 mVs^{-1} (Fig. S1A). The oxidation peak currents of AA increased gradually from pH 5 to pH 6.4 and then decreased until pH 7.4. Consequently, the anodic peak current I (μA) was the highest value at pH 6.4, so pH=6.4 was selected as the optimum supporting electrolyte that produces the highest catalytic pH supporting electrolyte.^{1, 2} Figure S1B shows that the AA redox peak potential shifted negatively with increasing pH from 5 to 7.4. By plotting the pH versus E (V), a linear relationship was obtained with regression equation $\text{pH} = 0.455 - 0.031 E(\text{V})$ with $R^2 = 0.931$, where the slope = 0.031 mV. The negative shift with varying pH of supporting electrolyte may relate to the proton sharing on the electrooxidation reaction of AA; moreover, the number of protons equals to the number of electrons evolved in the redox process, which is very close to the theoretical Nernst value of 59 mV.²⁻⁶

2.2 Scan rate effect of AA on S-MCMS-900-modified electrode

The electrochemical oxidation of AA at the S-MCMS-900-modified electrode with varying scan rates was investigated to evaluate the kinetic surface process using CV in 0.1 M PBS (pH 6.4) containing 0.5 mM AA. Figure S1C shows the CVs of S-MCMS-900 in 0.5 mM AA at varying scan rates from 20–300 mVs^{-1} , where the oxidation peak current increased with increasing scan rate. A linear relationship between the current and the scan rate was observed in the regression equation (I (μA) = $3.4 + 0.046v$

mVs^{-1}), $R^2 = 0.98$ (Fig. S1D). These results illustrate that the overall process of AA at the active sites of S-MCMS-900 is a typical controlled adsorption process.^{2, 4-6}

Figures

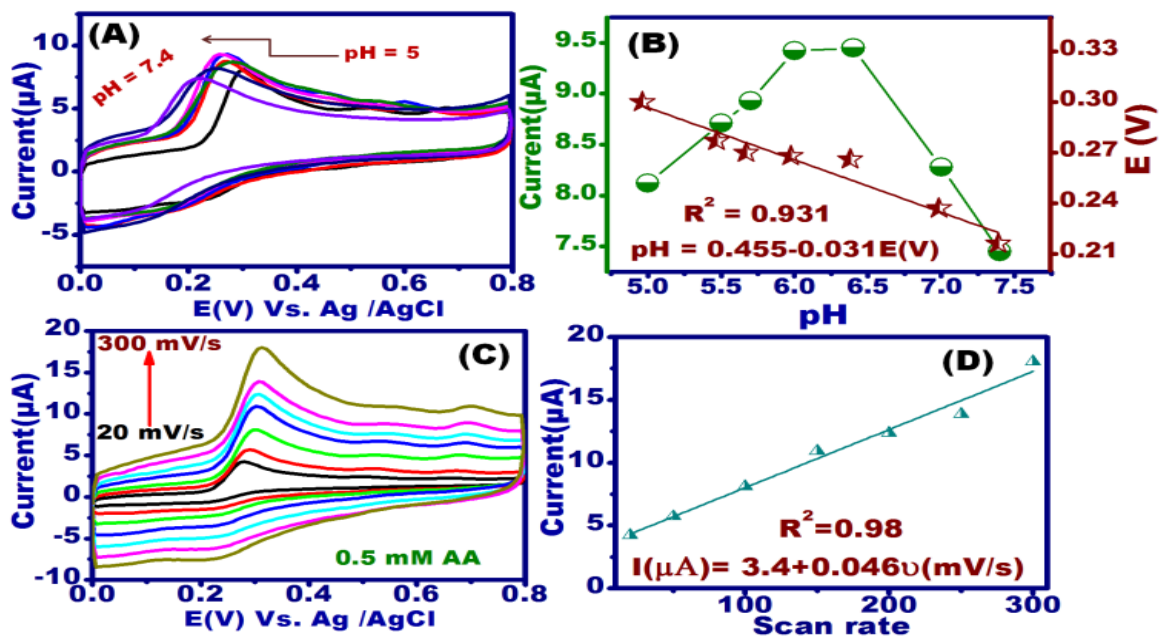
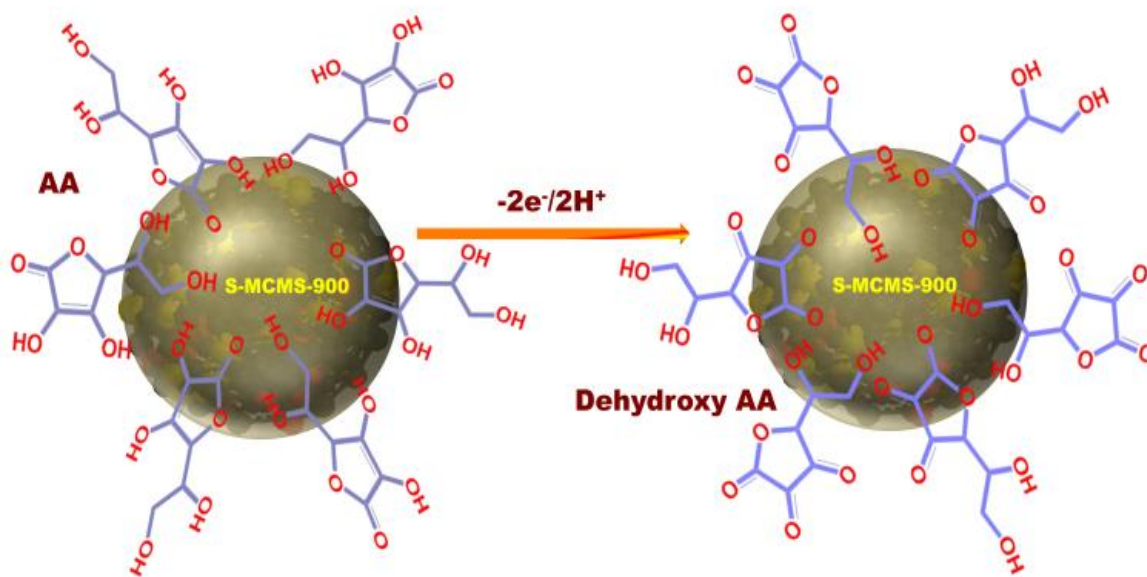


Figure S1. A) CVs of 0.5 mM AA at varying supporting electrolyte (PBS) pH values (5-7.4) at a scan rate of 100 mVs^{-1} on S-MCMS-900- modified electrode. B) The plot of pH versus the current values (μA) (olive scatter), and applied potential (V) (wine points). C) The CVs of 0.5 mM AA at varying scan rate (20-300 mVs^{-1}) in 0.1 M PBS (pH 6.4) on S-MCMS-900-modified electrode. D) The plot of scan rate (mVs^{-1}) vs the corresponding current (μA).



Scheme S1. The electro-oxidation mechanism of ascorbic acid (AA) at S-MCMS surfaces illustrates the oxidation of AA to dehydroxy-AA with losing of $2e^-/2H^+$.

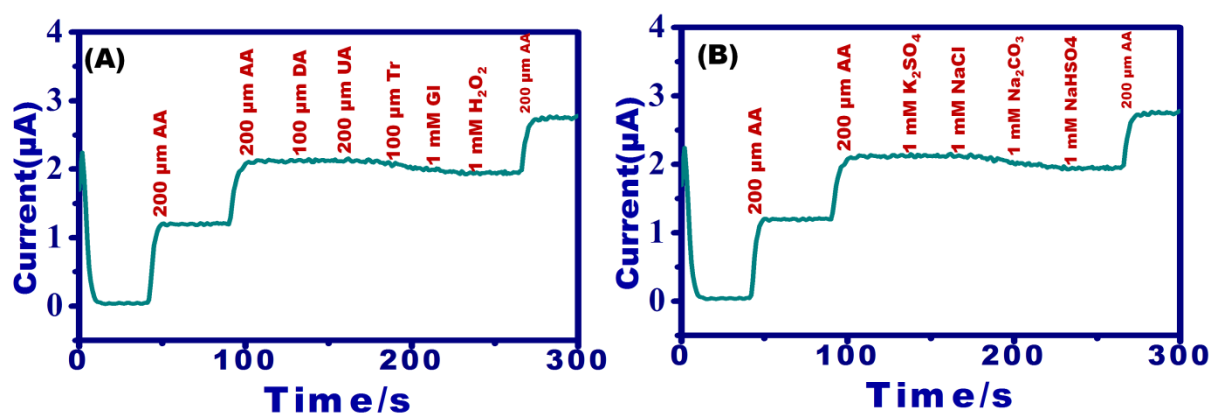


Figure S2. A) The amperometric response of 0.2 mM AA and other interfering molecules such as DA, UA, Tr, Gl, and H_2O_2 on the S-MCMS-900-modified electrode at honest applied potential 0.25 V in 0.1 M PBS (pH = 6.4). B) The amperometric response of 0.2 mM AA and other interfering salts such as K_2SO_4 , NaCl, Na_2CO_3 , and NaHSO₄ at honest applied potential 0.25 V in 0.1 M PBS (pH = 6.4).

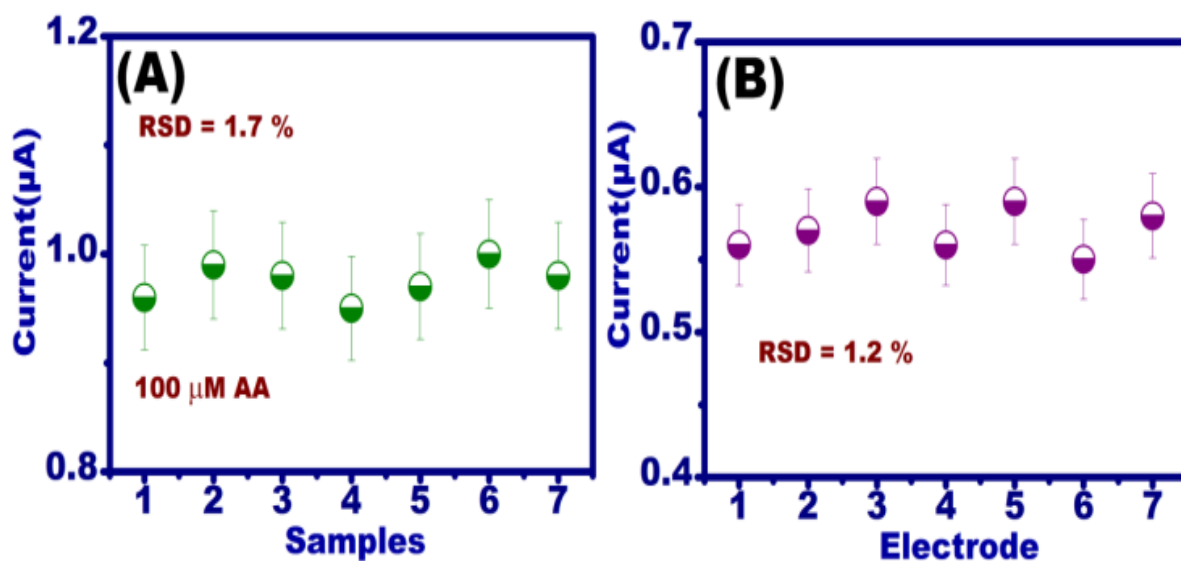


Figure S3. The stability of S-MCMS-900-modified electrode over 7 samples of 0.1 mM AA in 0.1 M PBS (pH 6.4) using SWV- measurements. B) The reproducibility of S-MCMS-900 over 7 electrodes of 0.1 mM AA in 0.1 M PBS (pH 6.4) using SWV-

Table S1. Comparison of the analytical performance of S-MCMS-900- modified electrode for monitoring of ascorbic acid with other modified electrodes as a function of detection limit and linear range.

Electrode	Ascorbic acid		References
	Linear range (mM)	Detection limit (μM)	
GSTG/Chitosan(Chit)/GCE ^a	3×10^{-4} - 10^{-2}	0.07	7
PdPt/CPE ^b	0.31-20	62	8
CA/DCPI-CME ^c	0.1-6	10	9
Co/Si(100)	0.1×10^{-3} – 10^{-2}	0.1	10
PdPt-BANS ^d	0.01-0.97	0.2	11

^a gold nanoparticle (AuNP)-modulated hydrophilic sodium dodecylsulfate (SDS)-wrapped graphene (G)-tolonium chloride (TC)/glassy carbon electrode.

^b palladium platinum/ carbon paste electrode

^c cellulose acetate polymeric film bearing 2,6-dichlorophenolindophenol

^d PdPt bimetallic alloy nanowires

References

1. b. Xiao-Bo Li a, Md. Mahbubur Rahman b, Guang-Ri Xu a, Jae-Joon Lee, *Electrochim. Acta* 2015, 173
2. H. Ibrahim and Y. Temerk, *J. Electroanal. Chem.* 2016, 780, 176-186.
3. Y. G. Yaru Li, Bo Zheng, Lan Luo, Cong Li, Xiaoyi Yan, Tingting Zhang, Nannan Lu, and Z. Zhang, *Talanta*, 2017, 162, 80–89.
4. N. Akhtar, M. Y. Emran, M. Shenashen, H. Khalifa, T. Osaka, A. Faheem, T. Homma, H. Kawarada and S. El-Safty, *J. Mater. Chem. B*, 2017, 5 (39), 7985-7996.
5. M. Emran, M. Mekawy, N. Akhtar, M. Shenashen, I. EL-Sewify, A. Faheem and S. El-Safty, *Biosens. Bioelectron.* 2018, 100, 122-131.
6. M. Y. Emran, H. Khalifa, H. Gomaa, M. A. Shenashen, N. Akhtar, M. Mekawy, A. Faheem and S. A. El-Safty, *Microchim. Acta*, 2017, 184 (11), 4553-4562
7. H. Kashyap, P. K. Singh, F. Verma, V. K. Rai, A. Rai and M. Singh, *New J. Chem.* 2017, 41, 6489-6496.
8. A. M. Pisoschi, A. Pop, G. P. Negulescu and A. Pisoschi, *Molecules*, 2011, 16, 1349-1365.
9. A. B. Florou, M. I. Prodromidis, M. I. Karayannis and S. M. Tzouwara-Karayanni, *Anal. Chim. Acta*, 2000, 409, 113-121.
10. L. Zhao, K. Liao, M. Pynenburg, L. Wong, N. Heinig, J. P. Thomas and K. Leung, *ACS Appl. mater. interfaces*, 2013, 5, 2410-2416.
11. L. Jin, Z. Zhang, Z. Zhuang, Z. Meng, C. Li and Y. Shen, *RSC Adv.* 2016, 6, 42008-42013.